

DOI: 10.1002/anie.200600545

**Multifunctional Lipid/Quantum Dot Hybrid Nanocontainers for Controlled Targeting of Live Cells\*\****Gopakumar Gopalakrishnan, Christophe Danelon, Paulina Izewska, Michael Prummer, Pierre-Yves Bolinger, Isabelle Geissbühler, Davide Demurtas, Jacques Dubochet, and Horst Vogel\**

Nanocrystal-based organic–inorganic functional hybrid materials with novel, exceptional properties have been explored in recent years because of their potential applications in nanobiotechnology.<sup>[1]</sup> Viral assembly of inorganic nanoparticles,<sup>[2a]</sup> and their polypeptide<sup>[2b,c]</sup> and ligand-receptor-mediated organization<sup>[2d]</sup> and protein-templated synthesis<sup>[2e]</sup> are a few examples in this direction. Of utmost interest in this context are lipid molecules because of their unique ability to form a variety of self-organized, supramolecular structures.<sup>[3]</sup> Although planar and vesicular lipid membranes have been used to compartmentalize and to synthesize nanocrystals in a confined volume,<sup>[4]</sup> the enormous possibilities of lipid-based, biocompatible nano/microstructures in nanobiotechnology have still to be fully exploited. For example, native and artificial vesicles offer novel possibilities for investigating (bio)chemical reactions and cellular signal transduction processes at the nanometer and attoliter scales.<sup>[5]</sup> Furthermore, the interaction between specially designed lipid vesicles and mammalian cells (adsorption, fusion, endocytosis)<sup>[6a]</sup> has been used to deliver DNA and RNA into cells, and has high potential for smart diagnostics, controlled drug delivery, and gene transfer.<sup>[4a,6]</sup> Inorganic nanoparticles could offer new ways to image native and artificial vesicles and control (bio)chemical reactions therein, if it is possible to selectively position the particles on or within the vesicles.

[\*] Dr. G. Gopalakrishnan, Dr. C. Danelon, P. Izewska, Dr. M. Prummer, P.-Y. Bolinger, Dr. I. Geissbühler, Prof. Dr. H. Vogel  
Laboratoire de Chimie Physique des Polymères et Membranes  
Institut des Sciences et Ingénierie Chimiques (ISIC)  
Ecole Polytechnique Fédérale de Lausanne (EPFL)  
1015 Lausanne (Switzerland)  
Fax: (+ 41) 21-693-6190  
E-mail: horst.vogel@epfl.ch

D. Demurtas, Prof. Dr. J. Dubochet  
Laboratoire d'Analyse Ultrastructurale (LAU)  
Université de Lausanne (UNIL)  
1015 Lausanne (Switzerland)

[\*\*] This work was supported by a grant (no. 4047-057562) from the NRP-47 program of the Swiss National Science Foundation and internal grants from the EPFL. We thank Marc Adrian (LAU, UNIL) for support with electron microscopy, and Ruud Hovius and Jean-Manuel Segura (LCPPM, EPFL) for helpful discussions.



Supporting information for this article is available on the WWW under <http://www.angewandte.org> or from the author.

In this context, we investigated quantum dots (QDs), which are inorganic, strongly fluorescent nanoparticles of exceptional photostability, for the *in vivo* imaging of cellular processes.<sup>[7]</sup> Notably, coating hydrophobic QDs with phospholipids is a generic method for making them water-soluble<sup>[8a]</sup> and biocompatible,<sup>[8b]</sup> which is useful for investigating biochemical reactions *in vitro*<sup>[9a]</sup> and when QDs are microinjected into live cells.<sup>[9b]</sup>

Herein, we report an interesting observation of wide-ranging potential for cellular imaging and manipulation: hydrophobic QDs can be readily incorporated into the bilayer membrane of lipid vesicles. Such lipid/QD hybrid vesicles (HVs) are capable of fusing with live cells, thereby staining a cell's plasma membrane selectively with fluorescent QDs and transferring the vesicle's cargo into the cell.

Figure 1a depicts the steps involved in the fabrication of the HVs. A solution of trioctylphosphine oxide (TOPO) coated CdSe QDs and lipids in chloroform is dried in a vial to

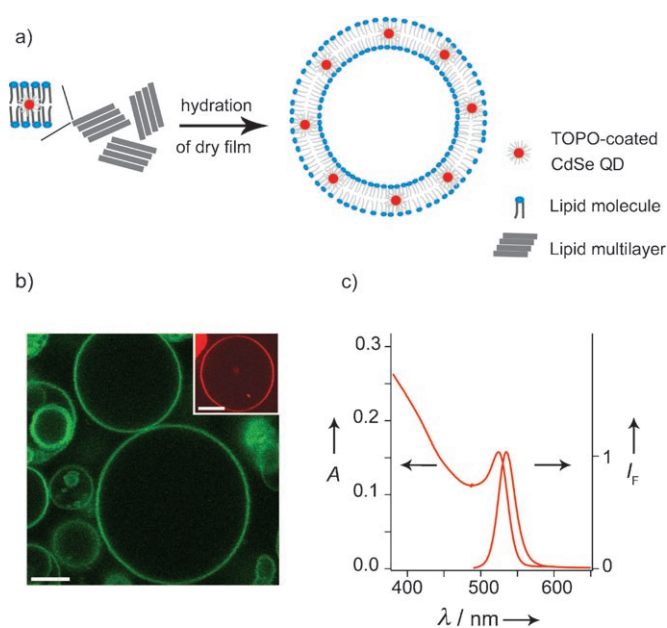


**Figure 1.** a) Steps involved in the formation of lipid/QD HVs. b) Confocal fluorescence cross-sectional image of HVs made of DMPC by hydration swelling. The inset shows vesicles stained with rhodamine-labeled lipids. Scale bars: 10  $\mu\text{m}$ . c) Typical absorption/emission spectra of the CdSe QDs used in the preparation of HVs. The narrow emission spectrum indicates the uniform size (ca. 3 nm) of the QDs.

form a multilamellar lipid film, from which vesicles are spontaneously formed by hydration under water. We investigated a wide range of phospholipid molecules (different head groups, various alkyl chain lengths, etc.) as well as different established methods of liposome formation (classical swelling, electroswelling).<sup>[10]</sup> We found that the formation of the HVs is not limited to any particular class of lipid<sup>[10c]</sup> and/or method of formation. HVs with sizes ranging from 50 nm to a few tens of micrometers can be produced in a controlled manner.

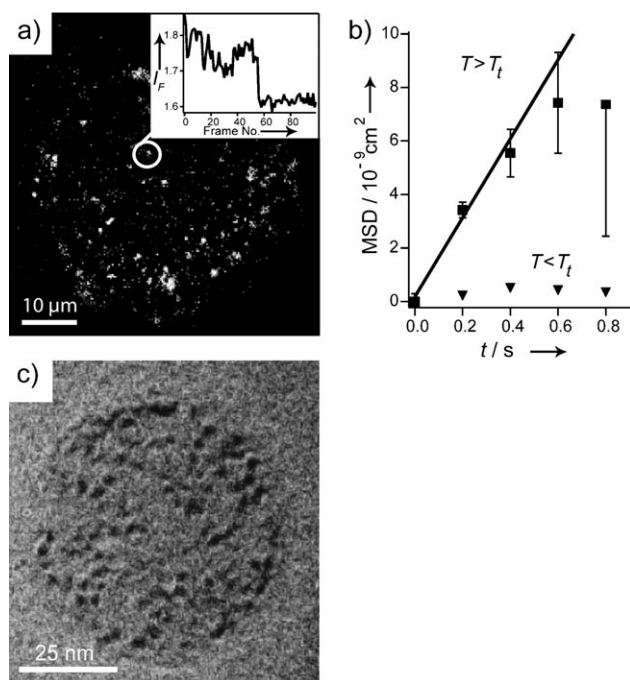
For ease of observation by confocal microscopy, we first fabricated giant vesicles (1–50  $\mu\text{m}$ ) by classical swelling.

Figure 1b shows representative confocal cross sections of vesicles, which appear as clear and sharp fluorescent circles at their perimeters. These images are comparable with those known to result from vesicles stained with fluorescent organic dyes,<sup>[10a]</sup> which are shown for comparison as the inset of Figure 1b. This result demonstrates that the hydrophobic QDs must be integrated in or attached to the lipid bilayer of the vesicle. A high yield of giant unilamellar vesicles was obtained along with some multilamellar ones, as is usually the case with this approach. Electroswelling<sup>[10b]</sup> produced more homogeneous unilamellar structures.

Figure 1c shows the absorption and emission spectra of the hydrophobic QDs employed in the production of the HVs. The spectral properties (position of maxima, narrow emission spectrum) indicate a uniform size of about 3 nm of the CdSe QD core;<sup>[11a,b]</sup> our TOPO/QDs have a size of about 5 nm, which includes the hydrophobic coating. Current limitations that result from photobleaching of organic membrane dyes in acquiring high-resolution images, thin *z*-sectioning for eventual 3D reconstruction, and longer-term *in situ* observations could be solved using our HVs. Although core-shell QDs<sup>[11c]</sup> offer higher photostability compared to core-only QDs, confocal imaging at higher laser power was performed uninterruptedly for hours using our TOPO-coated QDs.<sup>[11d]</sup> The imaging of vesicles, planar lipid bilayers, and lipid monolayers at the air/water interface can thus be performed for hours, which is of interest for studying phase diagrams and phase separation phenomena in lipid mixtures.<sup>[12,13]</sup>

Calorimetric measurements revealed the ordered-fluid phase transition temperature  $T_i$  of the lipid/QD vesicles at 23.5 °C, which is identical to that for pure DMPC bilayers.<sup>[3]</sup> This is actually not surprising considering that the lipid/QD molar ratio of our vesicles is 3000:1. Furthermore, we studied the lateral diffusion of QDs in the lipid bilayer above and below the  $T_i$  of giant vesicles of DMPC immobilized on a glass plate. Figure 2 shows fluorescence microscopy images of single QDs obtained from the planar membrane region of an immobilized vesicle in contact with a glass support. We observed substantially different diffusion of single QDs within the membrane below and above the  $T_i$  of the lipid bilayer. Figure 2a shows single QDs observed at 5 °C ( $< T_i$ ), with the inset giving a single-step photobleaching profile of an individual QD, which proves that the spots are single QDs (see also the movies in the Supporting Information). We calculated the lateral diffusion coefficient  $D$  from the mean-square displacements (MSDs) of the diffusing single QDs in the bilayer membrane, as described in Figure 2b and the Supporting Information. In the fluid lipid bilayer at 30 °C, the lateral diffusion of the QDs ( $D = 0.3 \times 10^{-8} \text{ cm}^2 \text{ s}^{-1}$ ) is about ten times slower than that of a lipid molecule ( $D = 4 \times 10^{-8} \text{ cm}^2 \text{ s}^{-1}$ );<sup>[12b,c]</sup> this reduced diffusion could be a result of the larger size of the QDs compared to lipid molecules. The actual diffusion coefficient might be slightly larger because of a systematic underestimation of fast particles by the single-particle-tracking algorithm.<sup>[14]</sup> In the fluid membrane phase, 75% of the tracked particles follow the diffusion profile whereas 25% are less mobile.

The tracked single QDs in the ordered bilayer state ( $T < T_i$ ) are nearly immobile, as revealed by the negligibly small



**Figure 2.** Imaging of single QDs in the bilayer of an immobilized giant vesicle. a) Fluorescence micrograph showing representative images of single QDs in the planar bilayer region attached to a glass surface at 5°C. The inset shows a photobleaching profile of a single QD. b) Calculated MSD values (mean of three experiments) of the trajectory of single QDs diffusing in a lipid bilayer are plotted as a function of time at 30°C for a fluid lipid bilayer (top) and at 5°C for an ordered lipid bilayer (bottom). From the MSD values, it is clear that QDs are immobile in the ordered lipid bilayer. The diffusion coefficient of QDs in the fluid lipid bilayer is calculated from the corresponding slope. (See the Supporting Information for movies of single-molecule experiments and for details of the MSD calculation.) c) Cryo-TEM image of a collapsed HV at ten times higher QD concentration than that used for the confocal microscopy images shown in Figure 1 b. The ca. 3-nm QDs (dark spots) are randomly distributed in the vesicle's lipid bilayer.

MSD values. It is important to mention here that the switching of the diffusion properties of the QDs occurs at exactly 23.5°C, which is identical to the lipid phase transition temperature observed in the calorimetric measurements. These observations show that the QDs are tightly associated with the lipid membrane, because otherwise there would be little or no effect with respect to the membrane state. It has been suggested that hydrophobic QDs could be incorporated into lipid bilayers and thereby achieve efficient phase transfer from organic to aqueous medium,<sup>[8a]</sup> thus allowing the *in vitro* study of membrane association by fluorescence resonance energy transfer (FRET).<sup>[8b]</sup> In spite of these experimental approaches, the prediction of the exact location of the QDs relative to a lipid bilayer remains a difficult task, where artifacts and overinterpretations have to be carefully avoided.<sup>[8a]</sup> For all the applications discussed herein, it is sufficient to know that the QDs are stably associated with the bilayer, irrespective of whether they are fully or only partially inserted in the lipid bilayer.

The interaction of the lipid/QD vesicles with living cells was tested for two different lipid compositions (Figure 3 a–g).

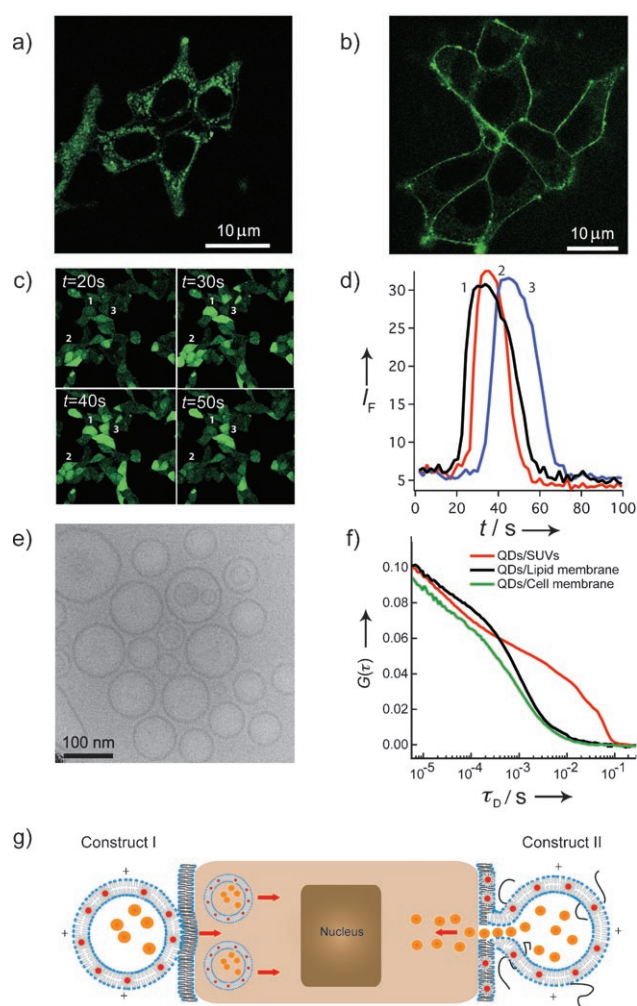


**Figure 3.** Interaction of HVs with HEK293 cells. a, b) Confocal micrographs of HEK293 cells 30 s after addition of vesicles: a) construct I vesicles are totally internalized into the cells; b) construct II vesicles selectively labeled the cell membrane without internalization into the cytoplasm. c) A series of confocal images (recorded at 300-ms scan rate) showing the fluorescence intensity response of Fluo-3 inside HEK293 cells at different times after fusion with construct II vesicles loaded with 1 mM CaCl<sub>2</sub>. d) The transient Fluo-3 fluorescence signals of a few representative cells (numbers correspond to numbered cells in (c)). e) Cryo-TEM image of construct II vesicles; the TEM images of construct I vesicles (not shown) are very similar. f) FCS autocorrelation curves showing diffusion times of QDs in different environments. The diffusion time of QDs in the cell plasma membrane observed after the fusion of HVs with the cell (green curve) is nearly identical to that in the lipid bilayer of an immobilized giant HV (black curve). The red curve shows the diffusion of small unilamellar vesicles (SUVs, 20–100 nm; construct II) in solution. g) Cartoon illustrating interactions of construct I and II HVs with living cells. Orange dots in the interior of the HVs represent any deliverable water-soluble molecules.

Construct I HVs are designed for transfer into the cell (Figure 3g). The bilayer of small HVs (20–100 nm; characterized by electron microscopy, as in Figure 3e) consists of 25% positively charged lipid (DOTAP), which is known to enhance the cellular internalization,<sup>[15]</sup> and 75% DMPC. Lipid/QD hybrid structures were found inside the cytosol within seconds after incubation with cells (Figure 3a). This

efficient uptake might allow further targeting of HVs to specific locations inside live cells through prior decoration of the HV surface with specific receptors.<sup>[16]</sup> Despite the universal use of cationic lipids in DNA transfection experiments,<sup>[15a]</sup> the exact mechanism of this event is still not clear.<sup>[17]</sup>

Construct II HVs were designed to fuse with the plasma membrane of a live cell (Figure 3g). This process is usually very difficult to achieve at room temperature.<sup>[18]</sup> As in the preceding experiment, small HVs (20–100 nm, Figure 3e) are used which now comprise 25% positively charged lipid (DOTAP), 0.5% DPPE-PEG2000, and 74.5% DMPC. Figure 3b shows a confocal image of live cells that were incubated with construct II vesicles. Interestingly, in this case the cell membrane is selectively labeled and no fluorescence was observed in the cytosol even after 1 h of incubation. The mechanism is not yet understood, but we speculate that the membrane-incorporated PEG molecules act as a transient barrier<sup>[19]</sup> between the cationic liposomal and anionic cellular membranes, thus preventing them from becoming internalized. At this distance (nanometer range), the collective process of electrostatic attraction (resulting from positively charged lipids) and membrane vulnerability (resulting from PE lipids and QDs) triggers the fusion between the membranes.

The appearance of QD fluorescence in the cellular membrane (Figure 3b) could be a consequence of either stable adhesion of intact vesicles on the surface of the plasma membrane or fusion between the bilayer of HVs and the plasma membrane, thus resulting in integration of the QDs into the cell membrane. For a better understanding of the exact event, the HVs were used as nanocontainers filled with aqueous  $\text{CaCl}_2$  and incubated with cells, which were loaded with Fluo-3 (a fluorescence indicator to measure the  $\text{Ca}^{2+}$  ion concentration in the cytoplasm). After a certain time lag the cells responded by a transient increase in intracellular  $\text{Ca}^{2+}$  ion concentration (Figure 3c,d), followed by selective labeling of the plasma membrane (similar to Figure 3b for an experiment without intracellular Fluo-3). The increase in intracellular  $\text{Ca}^{2+}$  concentration is transient because the  $\text{Ca}^{2+}$  vesicle cargo released into the living cells becomes accommodated in the endoplasmic reticulum by the cellular machinery. The following control experiments were performed to prove the fusion capability of the HV nanocontainers: 1) on addition of 1 mM  $\text{CaCl}_2$ /phosphate-buffered saline (PBS) without vesicles to the external medium of cells loaded with Fluo-3, the cells did not give an intracellular  $\text{Ca}^{2+}$  response; 2) addition of HV nanocontainers without a  $\text{CaCl}_2$  cargo to Fluo-3 loaded cells also did not induce an intracellular  $\text{Ca}^{2+}$  response. This result shows that the  $\text{Ca}^{2+}$  ions were not generated inside the cells through any kind of activation of intracellular  $\text{Ca}^{2+}$  ion stores upon vesicle interaction with the cellular membrane surface, but were delivered into the cell from the nanocontainers by fusion.

Fluorescence correlation spectroscopy (FCS) measurements were performed on the plasma membrane of live cells after incubating them with construct II vesicles to exclude any possibility that nanocontainers are simply adsorbed on the cell membrane, for example, by electrostatic interaction.

Figure 3f shows the measured autocorrelation functions (ACFs). The ACFs of QDs in the plasma membrane (green curve) and in the lipid bilayer of immobilized micrometer-sized HVs (black curve) are nearly identical, whereas the ACFs of a solution of small unilamellar vesicles show much slower diffusion (red curve). This finding demonstrates that the QDs reside within the plasma membrane of the cell, and gives additional proof that the observed cell membrane labeling and subsequent  $\text{Ca}^{2+}$  influx is caused by fusion between the vesicle bilayer and cell membrane. By using this approach, one can potentially carry any water-soluble material that can be enclosed inside the nanocontainers and deliver it into the live cells.

The use of QDs in biological cells always poses concerns about potential cytotoxicity. Unmodified TOPO-coated QDs are toxic to live cells,<sup>[20]</sup> probably by releasing  $\text{Cd}^{2+}$  ions into the cell as a result of poor surface coverage. Proper surface coating of QDs seems to avoid direct contact of the QD core with cells.<sup>[20]</sup> However, in our experiments the lipid/QD vesicles did not show any cytotoxic effects even after three hours of incubation with live cells. This finding indicates, but of course does not prove, that our QDs are well-embedded in the membrane rather than being in the membrane/water interfacial region. The *in vivo* experiments reported elsewhere using lipid-coated QDs<sup>[9b]</sup> also did not show any cytotoxic effects in embryonic cells, which suggests that lipid coating is an effective way to make QDs biocompatible.

Our results imply that cell and lipid membranes, and certainly the walls of polymeric vesicles,<sup>[21]</sup> can integrate any kind of hydrophobic nanoparticles whose size matches the membrane thickness.<sup>[10d]</sup> The incorporation of, for instance, nanometer-sized magnetic<sup>[22a–c]</sup> or metallic particles<sup>[23a]</sup> into the membranes will transform the properties of the cells or vesicles accordingly, and opens up novel possibilities for manipulating them as individuals or in ensembles with wide-ranging applications for nanoscale reactors,<sup>[5,24]</sup> cellular targeting,<sup>[25]</sup> targeted drug delivery,<sup>[26]</sup> contrast agents,<sup>[27]</sup> etc. The collective magnetic properties offered by the supra-molecular membrane systems will add complementary advantages compared to individual, biopolymer-modified, large magnetic nanoparticles.<sup>[22d]</sup> Another interesting field of investigation in the present context is Au nanoparticles; they are known for their thermal response to radio and photo irradiations, and presently receive great attention in photo/radiotherapy as magnetic particles in hyperthermia-aided diagnostics and treatment.<sup>[23b]</sup>

In summary, we have described the fabrication of highly controllable organic–inorganic HVs where nanometer-sized particles are confined to 4-nm-thick membranes. The tunable size, switchable physical properties, response to multiple external stimuli, and above all the controlled cell fusion capacity make them very promising tools in nanobiotechnology.

## Experimental Section

Lipids: 1,2-Dimyristoyl-*sn*-glycero-3-phosphatidylcholine (DMPC), 1,2-dioleoyl-3-trimethylammonium propane chloride salt (DOTAP), 1,2-distearoyl-*sn*-glycero-3-phosphatidylethanolamine-*N*-[biotinyl-

(polyethylene glycol 2000)] ammonium salt (DSPE-PEG2000-biotin), and 1,2-dipalmitoyl-*sn*-glycero-3-phosphatidylethanolamine-*N*-[methoxy(polyethylene glycol 2000)] ammonium salt (DPPE-PEG2000) were purchased from Avanti Polar Lipids.

Preparation of hybrid vesicles (HVs): 1) Classical swelling: Chloroform solutions of DMPC (1.5 mM, 100  $\mu$ L), DSPE-PEG2000-biotin (0.6 mM, 5  $\mu$ L), and CdSe/TOPO QDs (5  $\mu$ M, 10  $\mu$ L) were mixed and dried in a vacuum for 4 h in a teflon chamber. The film was then hydrated overnight at 37 °C by incubating with sucrose (0.1 M). 2) Electrowetting: Chloroform solutions of DMPC (1.5 mM, 100  $\mu$ L), DSPE-PEG2000-biotin (0.6 mM, 5  $\mu$ L), and CdSe/TOPO QDs (5  $\mu$ M, 10  $\mu$ L) were mixed and dried in a vacuum for 4 h on a glass slide coated with indium tin oxide (Sigma). The film was then hydrated at 37 °C by incubating with sucrose (0.1 M) and applying an alternating electric field of 1.2 V/10 Hz during the first 2 h for effective swelling, and then 2.0 V/4 Hz for the next hour for easy detachment of the formed vesicles. 3) Immobilization of HVs for confocal microscopy: Biotinylated HVs in sucrose (0.1 M) were incubated on a glass coverslip, which was pretreated with avidin (0.1 mg mL<sup>-1</sup>) in glucose (0.1 M). The glucose solution was used to keep the osmotic pressure balanced while allowing quick settling of sucrose-filled HVs.

Live-cell experiments: 1) Cell culture: Adherent human embryonic kidney cells (HEK293) were cultured in Dulbecco's Modified Eagle Medium (D-MEM; Gibco, Invitrogen, USA), supplemented with 2.2% fetal calf serum (Gibco), in a humidified 5% CO<sub>2</sub> atmosphere at 37 °C. Cells were split at regular intervals. For confocal microscopy, HEK293 cells were seeded into six-well plates (TPP, Trasadingen, Switzerland) containing 25-mm-diameter glass coverslips (Assistant, Germany), in culture medium (2 mL) containing 2.2% fetal calf serum. The cells were grown for 24 h at 37 °C, washed with PBS, and used for further experiments. 2) Cell/construct I vesicles: Chloroform solutions of DMPC (1.5 mM, 75  $\mu$ L), DOTAP (1.5 mM, 25  $\mu$ L), and CdSe/TOPO QDs (5  $\mu$ M, 10  $\mu$ L) were mixed and dried in a vacuum for 4 h, and the film was hydrated at 40 °C in PBS under vigorous mixing. The solution was then sonified in a bath sonifier for 10 s. This solution (10  $\mu$ L) of small (20–100 nm) vesicles was added to the cells suspended in PBS (500  $\mu$ L). 3) Cell/construct II vesicles: Chloroform solutions of DMPC (1.5 mM, 75  $\mu$ L), DOTAP (1.5 mM, 25  $\mu$ L), DPPE-PEG2000-PE (0.6 mM, 5  $\mu$ L), and CdSe/TOPO QDs (5  $\mu$ M, 10  $\mu$ L) were mixed and dried in a vacuum for 4 h. The film was hydrated at 40 °C in PBS under vigorous mixing, and the solution was sonified in a bath sonifier for 10 s. This solution (10  $\mu$ L) of small (20–100 nm) vesicles was added to the cells suspended in PBS (500  $\mu$ L). 4) Ca<sup>2+</sup> imaging experiments: For intracellular Ca<sup>2+</sup> signaling tests, HEK293 cells were grown on sterile microscope coverslips as described above. Cells were loaded with Fluo-3 dye (Molecular Probes, Invitrogen, USA) 24 h after seeding at 37 °C in D-MEM medium containing 2.2% fetal calf serum, by incubation in serum-free D-MEM medium containing Fluo-3 for 30 min at 37 °C. Thereafter, the Fluo-3 containing medium was replaced by D-MEM medium supplemented with 10% fetal calf serum and incubated for 30 min at 37 °C. Subsequently, dye-loaded cells were washed with PBS and subjected to Ca<sup>2+</sup> imaging. Construct II vesicles were prepared as explained above in CaCl<sub>2</sub>/PBS (1 mM). A solution (10  $\mu$ L) of such small (20–100 nm) vesicles loaded with CaCl<sub>2</sub> was applied to the cells suspended in PBS (500  $\mu$ L).

All the fluorescence images were recorded using a Zeiss LSM 510 confocal microscope (Carl Zeiss AG, Germany) with an excitation wavelength of 488 nm and an emission wavelength of > 505 nm.

Received: February 9, 2006

Revised: May 5, 2006

Published online: July 18, 2006

**Keywords:** lipids · nanoparticles · organic–inorganic hybrid materials · quantum dots · vesicles

- [1] a) *Biom mineralization: Chemical and Biochemical Perspectives* (Eds.: S. Mann, J. Webb, R. J. P. Williams), VCH, New York, **1989**; b) J. Aizenberg, A. Tkachenko, S. Weiner, L. Addadi, G. Hendler, *Nature* **2001**, *412*, 819; c) T. Douglas, *Science* **2003**, *299*, 1192; d) B. I. Ipe, C. M. Niemeyer, *Angew. Chem.* **2006**, *118*, 519; *Angew. Chem. Int. Ed.* **2006**, *45*, 504; e) C. M. Niemeyer, *Angew. Chem.* **2003**, *115*, 5974; *Angew. Chem. Int. Ed.* **2003**, *42*, 5796.
- [2] a) S.-W. Lee, C. Mao, C. E. Flynn, A. M. Belcher, *Science* **2002**, *296*, 892; b) S. R. Whaley, D. S. English, E. L. Hu, P. F. Barbara, A. M. Belcher, *Nature* **2000**, *405*, 665; c) M. S. Wong, J. N. Cha, K.-S. Choi, T. J. Deming, G. D. Stucky, *Nano Lett.* **2002**, *2*, 583; d) M. Bäuml, D. Stamou, J.-M. Segura, R. Hovius, H. Vogel, *Langmuir* **2004**, *20*, 3828; e) T. Douglas, M. Young, *Nature* **1998**, *393*, 152.
- [3] a) G. Ceve, D. Marsh, *Phospholipid Bilayers: Physical Principles and Models*, Wiley, New York, **1987**; b) R. B. Gennis, *Biomembranes: Molecular Structure and Function*, Springer, New York, **1989**; c) O. G. Mouritsen, *Life as a Matter of Fat: The Emerging Science of Lipidomics*, Springer, Heidelberg, **2005**.
- [4] a) J. H. Collier, P. B. Messersmith, *Annu. Rev. Mater. Res.* **2001**, *31*, 237; b) G. Gopalakrishnan, J.-M. Segura, D. Stamou, C. Gaillard, M. Gjoni, R. Hovius, K. J. Schenk, P. A. Stadelmann, H. Vogel, *Angew. Chem.* **2005**, *117*, 5037; *Angew. Chem. Int. Ed.* **2005**, *44*, 4957.
- [5] a) H. Pick, E. L. Schmidt, A.-P. Tairi, E. Ilegems, R. Hovius, H. Vogel, *J. Am. Chem. Soc.* **2005**, *127*, 2908; b) P.-Y. Bolinger, D. Stamou, H. Vogel, *J. Am. Chem. Soc.* **2004**, *126*, 8594; c) D. Stamou, C. Duschl, E. Delamar, H. Vogel, *Angew. Chem.* **2003**, *115*, 5738; *Angew. Chem. Int. Ed.* **2003**, *42*, 5580.
- [6] a) R. E. Pagano, J. N. Weinstein, *Annu. Rev. Biophys. Bioeng.* **1978**, *7*, 435; b) G. Gregoriadis, *Trends Biotechnol.* **1995**, *13*, 527; c) V. P. Torchilin, *Nat. Rev.* **2005**, *4*, 145; d) V. P. Torchilin, A. N. Lukyanov, Z. Gao, B. P. Sternberg, *Proc. Natl. Acad. Sci. USA* **2003**, *100*, 6039; e) J. Kunisawa, T. Masuda, K. Katayama, T. Yoshihawa, Y. Tsutsumi, M. Akashi, T. Mayumi, S. Nakagawa, *J. Controlled Release* **2005**, *105*, 344.
- [7] a) X. Michalet, F. F. Pinaud, L. A. Bentolila, J. M. Tsay, S. Doose, J. J. Li, G. Sundaresan, A. M. Wu, S. S. Gambhir, S. Weiss, *Science* **2005**, *307*, 538; b) X. Gao, L. Yang, J. A. Petros, F. F. Marshall, J. W. Simons, S. Nie, *Curr. Opin. Biotechnol.* **2005**, *16*, 63.
- [8] a) L. Feng, X. Kong, K. Chao, Y. Sun, Q. Zeng, Y. Zhang, *Mater. Chem. Phys.* **2005**, *93*, 310; We cite this report with reservations. 1) The authors claim to show the incorporation of QDs into lipid bilayers by electron and optical microscopy. However, the quality of their electron and optical micrographs does not allow localization of QDs inside or outside the lipid vesicles. 2) From differential scanning calorimetry experiments they claim that increasing amounts of QDs decrease the lipid phase-transition enthalpy, which they took as further proof of QD insertion into lipid bilayers: the reported enthalpy is ca. 0.08 J g<sup>-1</sup>, which is orders of magnitude smaller than that typically measured (ca. 35 J g<sup>-1</sup>) in lipid systems; b) J. A. Kloepper, N. Cohen, J. L. Nadeau, *J. Phys. Chem. B* **2004**, *108*, 17042.
- [9] a) I. Geissbuehler, R. Hovius, K. L. Martinez, M. Adrian, K. R. Thampi, H. Vogel, *Angew. Chem.* **2005**, *117*, 1412; *Angew. Chem. Int. Ed.* **2005**, *44*, 1388; b) B. Dubertret, P. Skourides, D. J. Norris, V. Noireaux, A. H. Brivanlou, A. Libchaber, *Science* **2002**, *298*, 1759.
- [10] a) K. Akashi, H. Miyata, H. Itoh, K. Kinoshita, *Biophys. J.* **1996**, *71*, 3242; b) M. I. Angelova, D. S. Dimitrov, *Faraday Discuss. Chem. Soc.* **1986**, *81*, 303; c) The HVs were prepared using saturated lipids such as DLPC, DMPC, DPPC, and DSPC, as well as unsaturated lipids such as DOPC and DOPG using classical swelling and electrowetting. The results imply that HV formation is not limited to any particular class of lipids used;

- d) Larger QDs (ca. 8 nm) were not integrated in the vesicle lipid bilayer under our experimental conditions; this size exclusion of ca. 5 nm is about the thickness of the lipid bilayer.
- [11] a) C. B. Murray, D. J. Norris, M. G. Bawendi, *J. Am. Chem. Soc.* **1993**, *115*, 8706; b) Z. A. Peng, X. G. Peng, *J. Am. Chem. Soc.* **2001**, *123*, 183; c) B. O. Dabbousi, J. RodriguezViejo, F. V. Mikulec, J. R. Heine, H. Mattoussi, R. Ober, K. F. Jensen, M. G. Bawendi, *J. Phys. Chem. B* **1997**, *101*, 9463; d) The quantum yield of the QDs was measured by standard methods and found to be 25%.
- [12] a) J. Korlach, P. Schwille, W. W. Webb, G. W. Feigenson, *Proc. Natl. Acad. Sci. USA* **1999**, *96*, 8641; b) A. E. Hac, H. M. Seeger, M. Fidorra, T. Heimburg, *Biophys. J.* **2005**, *88*, 317; c) L. A. Bagattoli, S. Sanchez, T. Hazlett, E. Gratton, *Methods Enzymol.* **2003**, *360*, 481.
- [13] a) H. Möhwald, *Annu. Rev. Phys. Chem.* **1990**, *41*, 441; b) H. M. McConnell, *Annu. Rev. Phys. Chem.* **1991**, *42*, 171; c) H. M. McConnell, M. Vrljic, *Annu. Rev. Biophys. Biomol. Struct.* **2003**, *32*, 469.
- [14] P. H. M. Lommerse, G. A. Blab, L. Cognet, G. S. Harms, B. E. S. Jagalska, H. P. Spaink, T. Schmidt, *Biophys. J.* **2004**, *86*, 69.
- [15] a) P. L. Felgner, T. R. Gadek, M. Holm, R. Roman, H. W. Chan, M. Wenz, J. P. Northrop, G. M. Ringold, M. Danielsen, *Proc. Natl. Acad. Sci. USA* **1987**, *84*, 7413; b) I. Wrobel, D. Collins, *Biochim. Biophys. Acta* **1995**, *1235*, 296.
- [16] a) K. S. Kawamura, M. Sung, E. Bolewska-Pedyczak, J. Gariépy, *Biochemistry* **2006**, *45*, 1116; b) S. Balayssac, F. Burlina, O. Convert, G. Bolbach, G. Chassaing, O. Lequin, *Biochemistry* **2006**, *45*, 1408.
- [17] a) S. Berezna, S. Schaefer, R. Heintzmann, M. Jahnz, G. Boese, A. Deniz, P. Schwille, *Biochim. Biophys. Acta* **1995**, *1235*, 296; b) A. L. Bailey, P. R. Cullis, *Biochemistry* **1997**, *36*, 1628.
- [18] a) E. H. Chen, E. N. Olson, *Science* **2005**, *308*, 369; b) S. J. Scales, M. F. A. Finley, R. H. Scheller, *Science* **2001**, *294*, 1015.
- [19] a) B. R. Lentz, *Chem. Phys. Lipids* **1994**, *73*, 91; b) S. W. Hui, T. L. Kuhl, Y. Q. Guo, J. Israelachvili, *Colloids Surf. B* **1999**, *14*, 213.
- [20] A. M. Derfus, W. C. W. Chan, S. N. Bhatia, *Nano Lett.* **2004**, *4*, 11.
- [21] a) P. Rigler, W. Meier, *J. Am. Chem. Soc.* **2006**, *128*, 367; b) D. E. Discher, A. Eisenberg, *Science* **2002**, *297*, 967.
- [22] a) S. Lecommandoux, O. Sandre, F. Chécot, J. R. Hernandez, R. Perzynski, *Adv. Mater.* **2005**, *17*, 712; b) H. Duan, D. Wang, D. G. Kurth, H. Möhwald, *Angew. Chem.* **2004**, *116*, 5757; *Angew. Chem. Int. Ed.* **2004**, *43*, 5639; c) J. Park, K. An, Y. Hwang, J. G. Park, H. J. Noh, J. Y. Kim, J. H. Park, N. M. Hwang, T. Hyeon, *Nat. Mater.* **2004**, *3*, 891; d) A. Ito, M. Shinkai, H. Honda, T. Kobayashi, *J. Biosci. Bioeng.* **2005**, *100*, 1.
- [23] a) C. Burda, X. Chen, R. Narayanan, M. A. El-Sayed, *Chem. Rev.* **2005**, *105*, 1025; b) P. Gangopadhyay, S. Gallet, E. Franz, A. Persoons, T. Verbiest, *IEEE Trans. Magn.* **2005**, *41*, 4194.
- [24] M. Karlsson, M. Davidson, R. Karlsson, A. Karlsson, J. Bergenholtz, Z. Konkoli, A. Jesorka, T. Lobovkina, J. Hurtig, M. Voinova, O. Orwar, *Annu. Rev. Phys. Chem.* **2004**, *55*, 613.
- [25] K. C. Crowder, M. S. Hughes, J. N. Marsh, A. M. Barbieri, R. W. Fuhrhop, G. M. Lanza, S. A. Wickline, *Ultrasound Med. Biol.* **2005**, *31*, 1693.
- [26] a) T. M. Allen, P. R. Cullis, *Science* **2004**, *303*, 1818; b) P. Broz, S. M. Benito, C. Saw, P. Burger, H. Heider, M. Pfisterer, S. Marsch, W. Meier, P. J. Hunziker, *J. Controlled Release* **2005**, *102*, 475.
- [27] a) G. J. Strijkens, W. J. M. Mulder, R. B. van Heeswijk, P. M. Frederik, P. Bomas, P. C. M. M. Magusin, K. Nicolay, *Magn. Reson. Mater. Phys. Biol. Med.* **2005**, *18*, 186; b) M. S. Martina, J. P. Forlin, C. Menager, O. Clement, G. Barratt, C. Grabielle-Madelmont, F. Gazeau, V. Cabuil, S. Lesieur, *J. Am. Chem. Soc.* **2005**, *127*, 10676.